ISSN 2354-9114 (online), ISSN 0024-9521 (print)
Indonesian Journal of Geography Vol 57, No.3 (2025): 448-464
DOI: 10.22146/ijg.101030 website: https://jurnal.ugm.ac.id/ijg

INDONESIAN JOURNAL OF GEOGRAPHY

RESEARCH ARTICLE

Climate Change Scenarios for Central Iran (2030-2100)

Seyyed Javad Sadatinejad[1*], Farshad Soleimani Sardoo[2], Mohammad Mirzavand[2*], Eko Haryono[3]

[1)] Natural Engineering Department, Faculty of Natural Resources, Jiroft University, Jiroft, Iran
[2)] School of Energy Engineering and Sustainable Resources, College of Interdisciplinary Science and Technology, University of Tehran, Tehran, Iran
[3)] Departemen Geografi Lingkungan, Fakultas Geografi, Universitas Gadjah Mada, Yogyakarta, Indonesia, Indonesia

Received: 2024-10-30
Revised: 2025-09-17
Accepted: 2025-11-16
Published: 2025-11-17

Key words: Climate Change; Central Plateau of Iran; RCP Scenarios; Rainfall Variability; Agricultural Resilience

Correspondent email : JSadatinejad@ut.ac.ir and MMirzavand@ut.ac.ir

Abstract This study examines the impact of climate change on key climatic parameters—temperature, rainfall, and wind speed—in Iran's central plateau, a region highly vulnerable to climate variability. Long-term data from major synoptic stations in Isfahan, Kerman, Yazd, and Semnan were analyzed using the Statistical Downscaling Model (SDSM) with the CanESM2 model. Future climate conditions were projected for the mid-century (2030–2060) and end-century (2070–2100) periods under RCP2.6, RCP4.5, and RCP8.5 scenarios. The analysis indicates a general warming trend across all stations, with changes in precipitation and wind speed that vary spatially. In the near future, some stations are expected to experience reduced rainfall and an average temperature increase of 1–2°C, while others may see slight precipitation increases. Wind speed trends also vary regionally. This study provides a comprehensive multi-variable assessment for a region with limited prior analysis, integrating projections for temperature, rainfall, and wind speed under multiple scenarios. Furthermore, this study is among the first to combine the SDSM and CanESM2 models to assess multi-variable climate change impacts in Iran's arid central plateau. The results offer a concise summary of anticipated climate changes, without providing detailed interpretation or policy recommendations, thereby establishing a solid foundation for further research and planning.

1. Introduction

Global warming, largely driven by industrialization and increasing greenhouse gas emissions, has profoundly altered climate systems and natural processes worldwide (Sutton et al., 2015; Hawkins et al., 2020). Recognizing human-induced climate change is essential for public awareness and adaptation, particularly where its impacts are substantial. Climate change poses serious threats to food security, agriculture, water resources, and ecosystems (Cetin et al., 2022; Marin et al., 2020; Varol et al., 2022), and its acceleration is increasingly evident (Cetin et al., 2023; Cevik Degerli and Cetin, 2023). Between 1906 and 2005, the global mean temperature increased by 0.74°C, with projections indicating continued warming throughout the 21st century (Tabari et al., 2011; Wang et al., 2007, 2013). Accurate climate projections are therefore critical for planning adaptation strategies. Climate models have steadily improved, with nearly half of the current models achieving spatial resolutions below 1.3° in both latitude and longitude, surpassing previous generations (Dupuis, 2007; Chen et al., 2013; Keerthirathne and Perera, 2015).

Temperature, rainfall, and wind speed are crucial parameters affecting agricultural productivity and water management (Erskine and Ashkar, 1993; Lobell et al., 2007; Cooper et al., 2008; Muchow et al., 1990). However, their temporal and spatial variability complicates trend detection (Sethi et al., 2015; Buba et al., 2013; Balyani et al., 2013). Downscaling approaches such as the Statistical Downscaling Model (SDSM), combined with general circulation models like HadCM3 and CanESM2, have been applied to project regional climate conditions under different emission scenarios (Chu et al., 2010; Mahmood and Babel, 2012). Studies in arid and semi-arid regions demonstrate that even modest changes in temperature and precipitation can substantially affect agriculture and water resources (Groisman et al., 2012; Almazroui et al., 2017).

The Central Plateau of Iran, encompassing major urban centers such as Isfahan, Yazd, Semnan, and Kerman, is characterized by arid to semi-arid conditions and high vulnerability to climate change. Limited water resources, reliance on agriculture, and fragile ecosystems exacerbate the impacts of increasing temperatures, shifting precipitation patterns, and variable wind regimes (Tabari et al., 2015; Azadi et al., 2018; Shaban et al., 2021). Urban centers face additional pressures from growing populations and rising demand for resources, making infrastructure resilience and urban planning crucial under changing climate conditions. Despite these vulnerabilities, few studies have conducted comprehensive multi-variable assessments of climate change impacts in this region. Previous research has often focused on single variables or lacked high-resolution, simultaneous modeling of temperature, rainfall, and wind speed. Although numerous global climate studies have been conducted, long-term prediction studies using downscaling in the Central Plateau of Iran remain limited, particularly those combining

temperature, rainfall, and wind speed parameters. This leaves a clear research gap in understanding how multi-variable climatic changes will affect agriculture, water availability, urban planning, and ecosystems. Addressing this gap is essential to guide sustainable resource management and adaptation strategies.

Therefore, the objective of this study is to model key climatic parameters—temperature, rainfall, and wind speed—and assess their future trends in the Central Plateau of Iran. Long-term data from major stations in Isfahan, Kerman, Yazd, and Semnan were used, with projections generated using the SDSM and CanESM2 models under multiple Representative Concentration Pathway (RCP) scenarios.

The novelty of this research lies in providing a comprehensive multi-variable assessment for a region with limited prior analysis, integrating projections of multiple climatic parameters to support sustainable agriculture, water management, urban planning, and ecosystem protection. By focusing on this region, the study contributes to refining climate models for semi-arid areas and provides actionable insights for policymakers to enhance resilience against climate-induced risks.

2. Methods

2.1. Study area and data

The central plateau of Iran, which covers over half of the country's area, is characterized by arid and semi-arid conditions. Annual precipitation in this region is low, averaging no more than 100 mm, often around 50 mm, and in some cases as little as 25 mm per year. In contrast, the region experiences high potential evaporation due to intense heat and sunlight, often exceeding 4,000 mm per year, making evaporation rates 40 to 80 times greater than annual precipitation. The average relative humidity ranges from 30 to 40 percent, dropping to as low as 15 percent during the warm season. Average annual temperatures vary between 15°C and 30°C, with recorded extremes ranging from a maximum of 51°C to a minimum of -18°C. The geographical location of the study area is shown in Figure 1. Two main datasets were used in this study. Historical observational data (daily rainfall, average temperature, and wind speed) obtained from synoptic stations across the Central Plateau of Iran for the period 1965–2017. CanESM2 model data, including large-scale predictors and reanalyzed atmospheric variables (NCEP), covering the period 1961–2005 for calibration and 2006–2100 for future scenario projections. The Isfahan, Yazd, Kerman, and Semnan stations were chosen because they (1) are major synoptic stations with long-term, continuous, and high-quality climate records; (2) represent different climatic subzones of the Central Plateau (semi-arid, arid, and hyper-arid conditions); and (3) are spatially well distributed, providing balanced geographic coverage of the region.

2.2. Methods

2.2.1. Downscaling approach (SDSM + CanESM2)

Since bias correction of general circulation model outputs requires long-term data, synoptic stations with extended historical records were selected for input into the SDSM model. Downscaling was performed using SDSM version 5.3, while the CanESM2 model outputs were processed using MATLAB R2021b and Microsoft Excel 2019**.** Table 1 provides details of the selected stations. After verifying and ensuring the quality of the observational data, NCEP reanalysis predictor variables with the highest correlation to the observational data were chosen. The number of NCEP predictor variables correlated with the observational data depends on the length of the statistical period and the type of process (conditional or unconditional). Generally, the longer the statistical period and the more continuous the variable (unconditional process), the fewer correlated variables are needed, resulting in more accurate modeling.

The SDSM method is based on the empirical/statistical relationship between large-scale variables from general circulation models (GCMs) and local variables (Wetterhall et al., 2006). This relationship is expressed as follows (Dibike and Coulibaly, 2005) (Eq.1):

$$Y=F(X) \quad \text{..... (1)}$$

Where Y is the predictor variable, X is the predicted variable, and f represents the transfer function, which is derived empirically from observational data. In this method, climatic variables at the global scale—such as mean sea level pressure, temperature, and geopotential height—are linked with local-scale variables, including precipitation and observed temperature. Statistical downscaling has been utilized not only for numerical

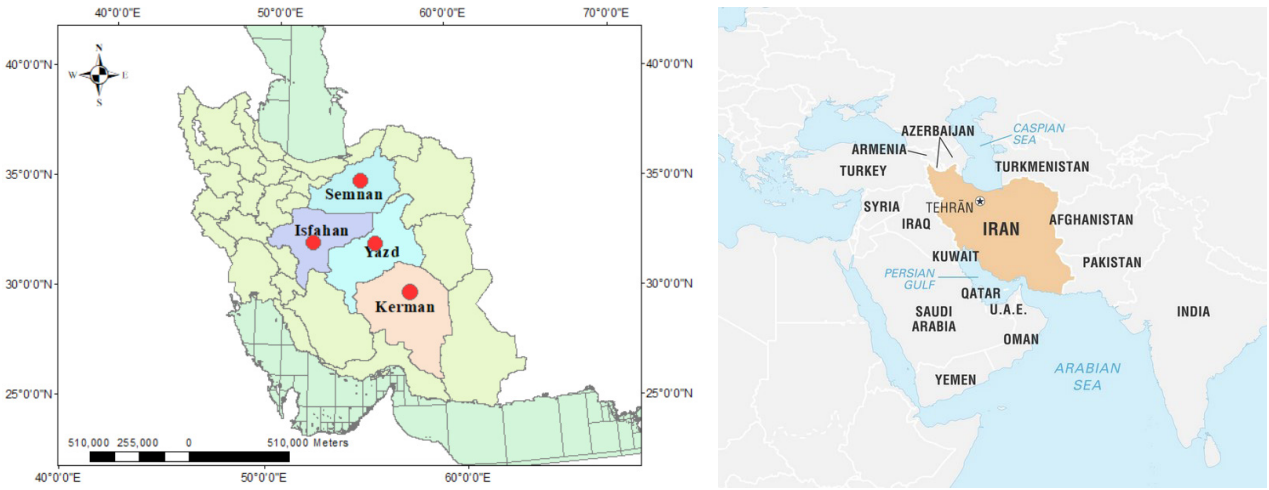

Figure 1. Geographic locations of the study area stations (red circles)

Table 1. Specifications of Synoptic Stations with Long-Term Statistical Records in the Study Area.

Station	Longitude	Latitude	Average rainfall (mm/year)	Average temperature (°C)	Mean wind speed (m/s)
Isfahan	29.08	58.45	122.05	16.69	1.67
Kerman	31.30	54.10	134.41	16.08	2.84
Semnan	30.58	53.08	137.95	18.47	1.69
Yazd	35.27	59.22	57.3	20.12	2.47

Table 2. Model Evaluation Criteria for Assessing Model Efficiency (Gupta et al.,1999; Chu and Shirmohammadi, 2004; Singh et al., 2004; Vasquez-Amábile and Engel, 2005)

Evaluation Criteria				Evaluation
The correlation coefficient	RSR	PBIAS	NSE	
0.86ρ<1	0RSR0.5	PBIAS$\pm$10	0.75<NSE1	Very good
0.73ρ<0.86	0.5<RSR0.6	$\pm$10PBIAS$\pm$15	0.65<NSE0.75	Good
0.6ρ<0.73	0.6<RSR0.7	$\pm$15PBIAS$\pm$25	0.5<NSE0.65	Acceptable
ρ<0.6	RSR>0.7	PBIAS>$\pm$25	NSE<0.5	Unacceptable

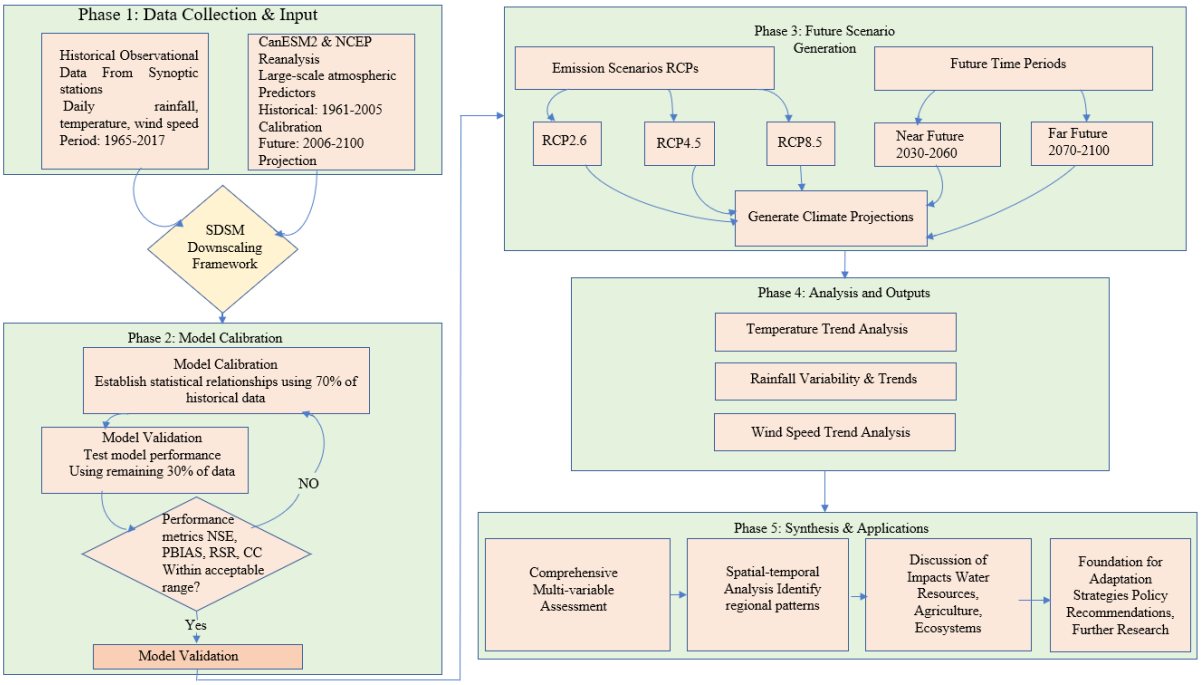

Figure 1. A Methodological Framework for Multi-Variable Climate Projection.

weather prediction and synoptic climatology but also for a wide range of climate application programs. The primary advantage of this statistical approach is its ability to evaluate the effects of climate change at the local level. The SDSM method has been extensively employed to downscale climate variables and assess hydrological responses under various climate change scenarios (Huang et al., 2011). SDSM integrates multiple linear regression with statistical air and climate data (Gebremeskel et al., 2005; Diaz-Nieto and Wilby, 2005; Gagnon et al., 2005; Wilby et al., 2007). In this study, SDSM version 5.3 was used for downscaling rainfall, temperature, and wind speed data. The method consists of four main components: determining NCEP predictor variables, model recalibration, model validation, and scenario generation and simulation for future periods (Sada, 2015).

To model daily climate data, it is essential to identify NCEP variables that have a logical and relevant relationship with the selected climate parameters. The output of the SDSM model is significantly influenced by the appropriate selection of these NCEP variables. Choosing the most suitable NCEP variable in the SDSM model is based on the coefficient of determination (R^2), the partial correlation coefficient, and the distribution

plots of the NCEP variables against the observed variable.

As mentioned, global circulation models (GCMs) are the primary tools for predicting changes and fluctuations in climate variables at both global and continental levels. In this study, we utilized the second generation of the Canadian Earth System Model, or CanESM2. This model is an enhanced version of the broader category of models known as Earth System Models (ESMs), which aim to incorporate the most significant components of land systems into their structure. While GCMs are effective for forecasting future climate changes, their outputs are based on large-scale grids ranging from 250 to 600 km (Gebremeskel et al., 2005). Due to the low spatial resolution of these global models, their outputs are not suitable for investigating the effects of climate change on a local scale. Downscaling is the most appropriate method for establishing the relationship between regional scales and large GCM models, with the regional scale defined as 50 x 50 km. Various methods have been developed for downscaling that address the discrepancies between global and regional scales. In this study, the SDSM statistical method was employed to downscale the output of the CanESM2 GCM.

Three types of inputs are used to model climate variables with the CanESM2 model: daily rainfall data, average temperature and wind speed from synoptic stations, and reanalyzed atmospheric data (NCEP), along with data from the CanESM2 model itself. The daily observational data are referred to as "predicted" variables, while the reanalyzed atmospheric data are labeled as "observational predictors," and the general circulation model data are termed "large-scale predictors." The observational and large-scale predictive datasets comprise 26 variables that are available for two key periods: from 1961 to 2005 and for the future period from 2006 to 2100.

2.2.2. Model Calibration

To develop the model, 70% of the observational data was used for calibration to determine the key parameters for rainfall, temperature, and wind speed. These parameters were then applied to the remaining 30% of the data for validation. The analysis is restricted to stations where the model output showed strong agreement with actual observations. We assessed model efficiency and uncertainty using several statistical metrics—including the Nash-Sutcliffe coefficient and percentage bias—against the acceptable criteria in Table 2. The subsequent sections provide a detailed discussion of the validation outcomes.

2.2.3. Scenario simulation (RCP2.6, RCP4.5, RCP8.5)

Following the baseline period modeling and evaluation, future climate projections were run for the near (2030–2060) and far future (2070–2100) under the RCP2.6, RCP4.5, and RCP8.5 scenarios.

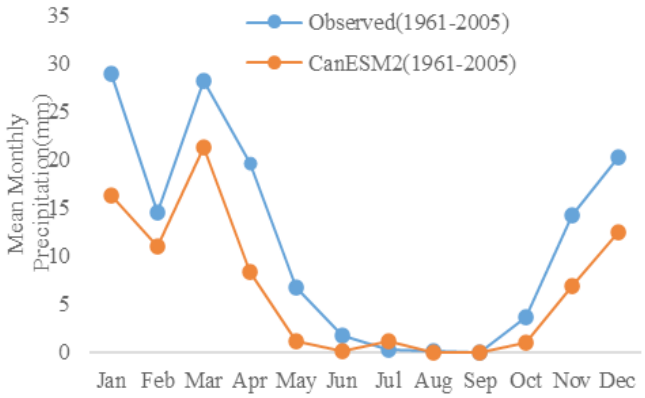

Figure 2. Comparison of Downscaled Rainfall Values from the CanESM2 Model with Observed Precipitation Data at Isfahan Station.

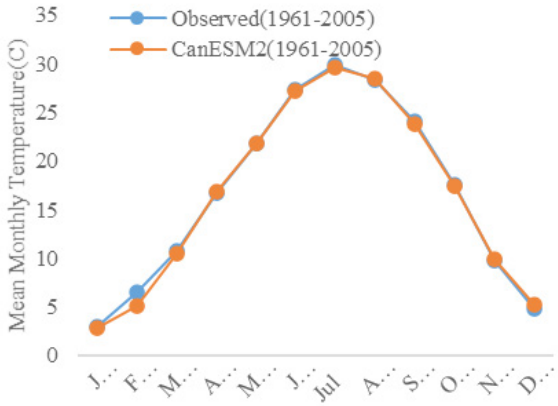

Figure 3. Comparison of Downscaled Mean Temperature Values from the CanESM2 Model with Observed Data at Isfahan Station.

Table 3. Evaluation Criteria for the CanESM2 Model: Rainfall, Average Temperature, and Wind Speed at Isfahan Station.

parameter	correlation coefficient	NRMSE	PBIAS	RSR	NSE
precipitation	0.85	0.08	20.7	0.69	0.513
temperature	0.99	0.01	0.88	0.05	0.997
Wind speed	0.96	0.06	-7.39	0.40	0.837

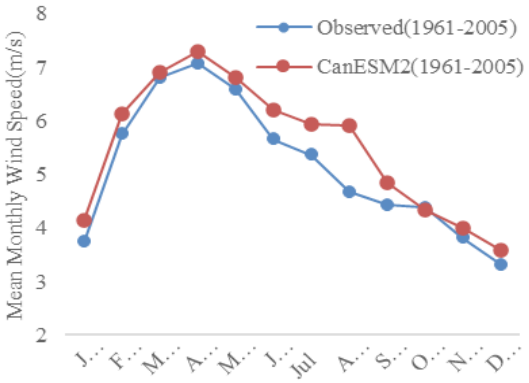

Figure 4. Comparison of Downscaled Wind Speed Values from the CanESM2 Model with Observed Data at Isfahan Station.

3. Result and Discussion

3.1. Model Validation

3.1.1. Isfahan Station

Figures 2 through 4 show monthly mean precipitation, mean temperature, and wind speed produced by the climate model, alongside observed data from the Isfahan station for the period 1961–2005. The downscaled rainfall predictions align closely with observed data, with only minor discrepancies in January and December (Figure 2). Evaluation criteria results confirm that the model performs efficiently within an acceptable range for simulating future rainfall at the Isfahan station (Table 3). The comparison of mean temperature values with observed data demonstrates the climate model's ability to accurately reproduce temperature trends at the Isfahan station (Figure 3). The model's temperature data aligns closely with observed values in nearly all months. Evaluation criteria further validate the CanESM2 model's effectiveness in simulating temperature at the Isfahan station (Table 3). The climate model's average wind speed values show strong alignment with observed data, with only a slight overestimation in August (Figure 4). Model evaluation further confirms the CanESM2 model's reliability in projecting future wind speed data (Table 3).

3.1.2. Kerman station

Monthly mean precipitation, mean temperature, and wind speed generated by the downscaled climate model, using observed data from the Kerman station during the period 1961–2005, are shown in Figures 5–7. The simulated rainfall values show good agreement with observed data (Figure 5), and the model evaluation criteria confirm the CanESM2 model's effectiveness in simulating rainfall (Table 4). Similarly, a comparison between modeled average temperature values and observations demonstrates that the climate model performs well in capturing temperature trends at the Kerman station (Figure 6). Most modeled temperature data are consistent with observed values, and model evaluation criteria indicate the CanESM2 model's strong suitability for temperature simulation at Kerman station (Table 4). For wind speed, the model's values align closely with observed data, with only a notable discrepancy in August (Figure 7). Model evaluation further supports the CanESM2 model's reliability in projecting wind speed for future periods at Kerman station (Table 4).

3.1.3. Semnan Station

Figures 8–10 present monthly mean precipitation, average temperature, and wind speed generated by the

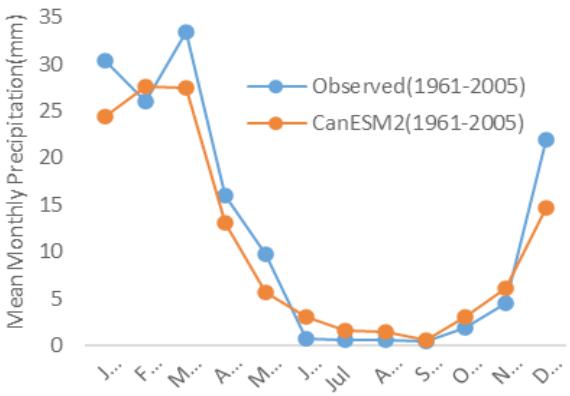

Figure 5. Comparison of Downscaled Rainfall Values from the CanESM2 Model with Observed Data at Kerman Station.

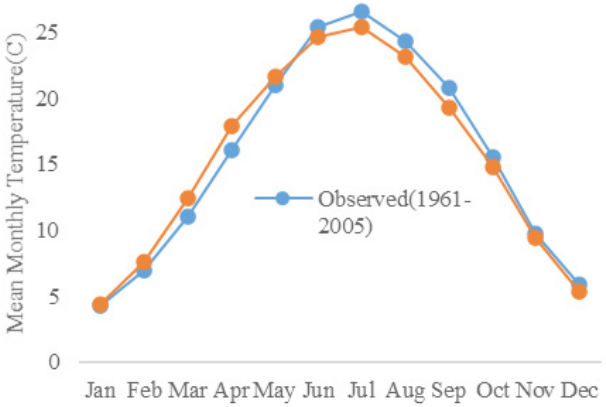

Figure 6. Comparison of Downscaled Average Temperature Values from the CanESM2 Model with Observed Data at Kerman Station.

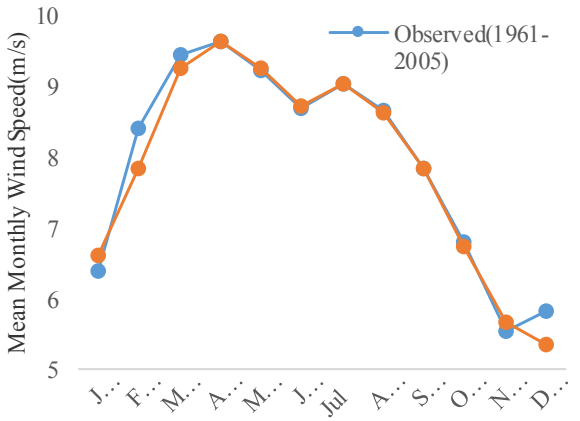

Figure 7. Comparison of Downscaled Wind Speed Values from the CanESM2 Model with Observed Data at Kerman Station.

Table 4. Evaluation Criteria for the CanESM2 Model: Rainfall, Average Temperature, and Wind Speed at Kerman Station.

Parameter	Correlation Coefficient	NRMSE	PBIAS	RSR	NSE
Precipitation	0.84	0.05	-18.57	0.70	0.55
Temperature	0.96	0.04	5.77	0.18	0.96
Wind speed	0.99	0.01	0.18	0.15	0.96

climate model, alongside observed data from the Semnan station for the period 1965–2005. The model's rainfall predictions align relatively well with observed data, though they are higher in March, April, and July (Figure 8). Evaluation criteria confirm the CanESM2 model's capability to simulate future rainfall at the Semnan station (Table 5). A comparison of the model's mean temperature values with observations indicates that the climate model performs well in simulating temperature at the Semnan station (Figure 9). Model performance metrics—Nash-Sutcliffe coefficient, normalized root mean square error, bias percentage, standard ratio, and correlation coefficient—all fall within the "very good" range for temperature (Table 5). For wind speed, however, the CanESM2 model produces values that exceed observed data (Figure 10). The evaluation criteria suggest that the CanESM2 model is less reliable for wind speed simulation at the Semnan station (Table 5).

3.1.4.Yazd station

Figures 11–13 illustrate monthly mean precipitation, average temperature, and wind speed generated by the climate model, alongside observed data from the Yazd station for the period 1961–2005. The predicted rainfall values generally align well with the observed data, although the model shows lower values than observed from January to March (Figure 11). Additionally, evaluation criteria confirm the CanESM2 model's capability to simulate future rainfall at the Yazd station (Table 6). A comparison of the model's mean temperature values with observed data indicates that the climate model has strong potential for accurately producing temperature data at the Yazd station (Figure 12). The model performance evaluation criteria further support the suitability of the CanESM2 model for temperature simulation in this region (Table 6). In terms of wind speed, the model's predictions are in good agreement with observed data at the Yazd station (Figure 13). However, the model generates higher wind speeds than observed during April and May. Overall, model evaluation confirms the CanESM2 model's effective performance in simulating wind speed for future periods (Table 6).

Generally,The performance of the CanESM2 model downscaled with SDSM was evaluated for four stations (Isfahan, Kerman, Semnan, Yazd) using historical data (1961–2005 for most stations; 1965–2005 for Semnan). Model evaluation focused on precipitation, temperature, and wind speed

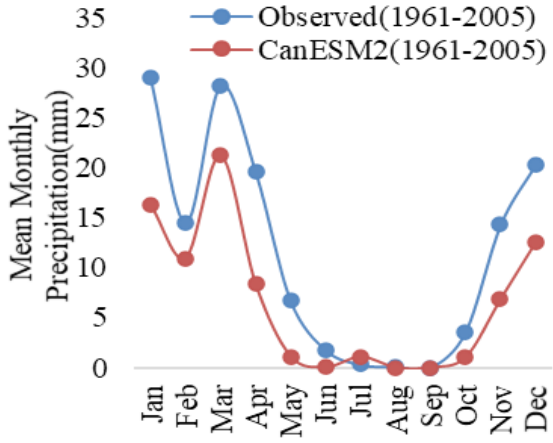

Figure 8. Comparison of Downscaled Rainfall Values from the CanESM2 Model with Observed Data at Semnan Station.

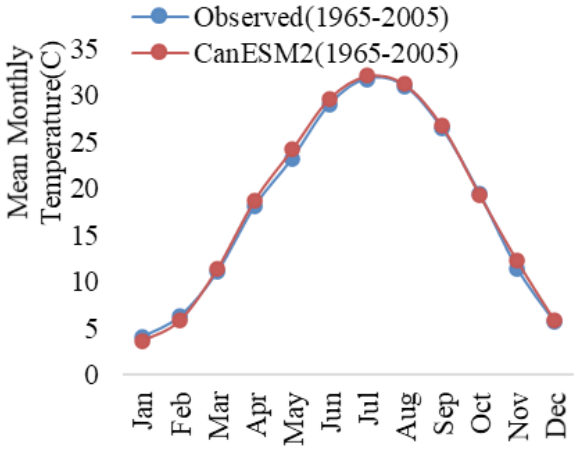

Figure 9. Comparison of Downscaled Temperature Values from the CanESM2 Model with Observed Data at Semnan Station.

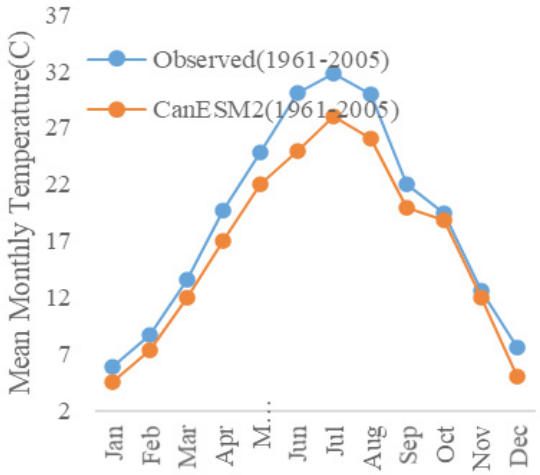

Figure 10. Comparison of Downscaled Wind Speed Values from the CanESM2 Model with Observed Data at Semnan Station.

Table 4. Evaluation Criteria for the CanESM2 Model: Rainfall, Average Temperature, and Wind Speed at Kerman Station.

parameter	correlation coefficient	NSE	RSR	PBIAS	NRMSE
Precipitation	0.60	0.63	21.23	0.06	0.87
Temperature	0.99	0.69	-1.65	0.01	0.99
Wind sped	0.23	0.71	38.13	0.40	0.24

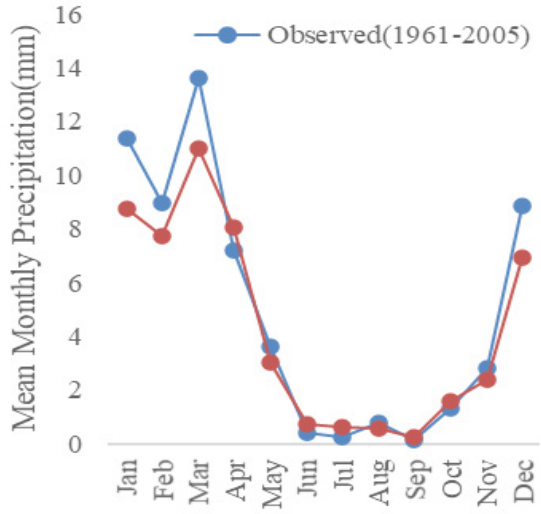

Figure 11. Comparison of Downscaled Rainfall Values from the CanESM2 Model with Observed Data at Yazd Station.

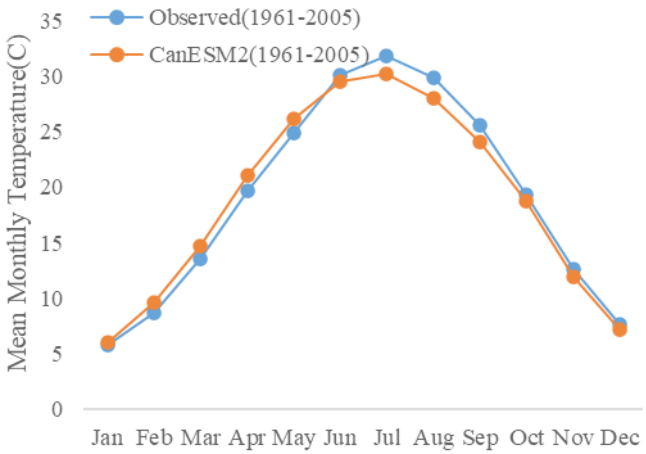

Figure 12. Comparison of Downscaled Mean Temperature Values from the CanESM2 Model with Observed Data at Yazd Station.

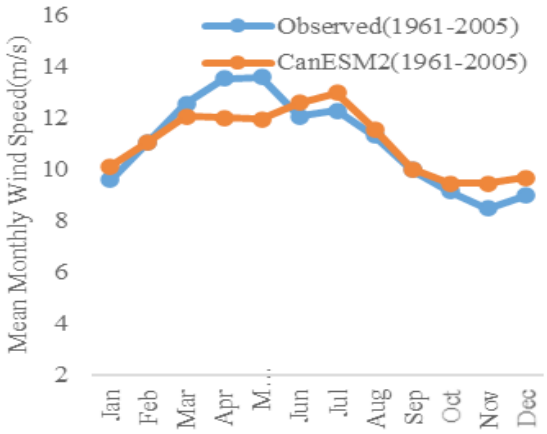

Figure 13 - comparison of downscaled values by CanESM2 model and wind speed observations of Yazd station.

Table 6. Evaluation Criteria for the CanESM2 Model: Rainfall, Average Temperature, and Wind Speed at Yazd Station.

parameter	correlation coefficient	NRMSE	PBIAS	RSR	NSE
precipitation	0.88	0.09	13	0.28	0.81
temperature	0.98	0.04	1.63	0.18	0.96
Wind Speed	0.87	0.04	-0.28	0.47	0.78

Table 1. Summary of Model Validation Metrics for All Stations

Station	Précipitation (CC / NSE)	Température (CC / NSE)	Wind Speed (CC / NSE)	Remarks
Isfahan	0.85 / 0.513	0.99 / 0.997	0.96 / 0.837	Minor Jan & Dec rainfall discrepancy
Kerman	0.84 / 0.55	0.96 / 0.96	0.99 / 0.96	Slight wind discrepancy in Aug
Semnan	0.60 / 0.63	0.99 / 0.69	0.23 / 0.24	Wind less reliable
Yazd	0.88 / 0.81	0.98 / 0.96	0.87 / 0.78	Slight low rainfall Jan–Mar, high wind Apr–May

3.2. Scenario Generation and Simulation of Climatic Parameters

Following the successful modeling and evaluation of the baseline period, future climate conditions were simulated for the near future (2030–2060) and the far future (2070–2100) under the RCP2.6, RCP4.5, and RCP8.5 scenarios.

3.2.1. Isfahan Station

Based on the projections for the Isfahan station, detailed in Figures 14 through 19 and quantified against the historical period (1961-2017) in Tables 7 to 9, the future climate is expected to shift significantly. Under the RCP scenarios, the annual average rainfall is projected to decrease. For the near future (2030–2060), rainfall is estimated at 92.2 mm, 92.1 mm, and 111.75 mm, representing decreases of 24.46%, 24.51%, and 8.44%, respectively, from the historical average of 122.05 mm. This declining trend continues into the far future (2070–2100), with projected rainfall of 92.22 mm, 87.09 mm, and 116.5 mm, resulting in further reductions of 24.44%, 28.65%, and 4.55%. Conversely, a substantial

warming trend is forecast. The average temperature is projected to rise to 17.42°C, 17.71°C, and 18.13°C in the near future, which corresponds to increases of 4.39%, 6.12%, and 8.62% above the historical average of 16.69°C. This warming intensifies dramatically in the far future, with temperatures expected to reach 17.53°C, 18.47°C, and 20.44°C—increases of 5.03%, 10.65%, and 22.43%, respectively. Finally, wind speed at the station is also predicted to increase slightly in the near future, with rises of 1.03%, 1.15%, and 1.4% under the RCP scenarios.

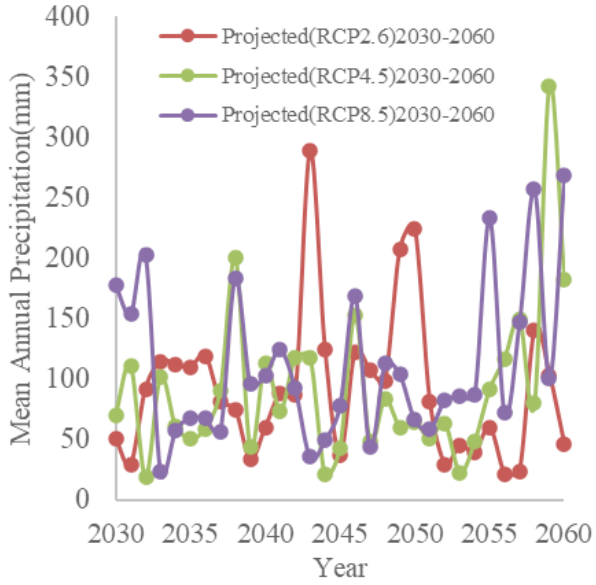

Figure 14. Simulated Rainfall Values for the Near Future Period (2030–2060) at Isfahan Station.

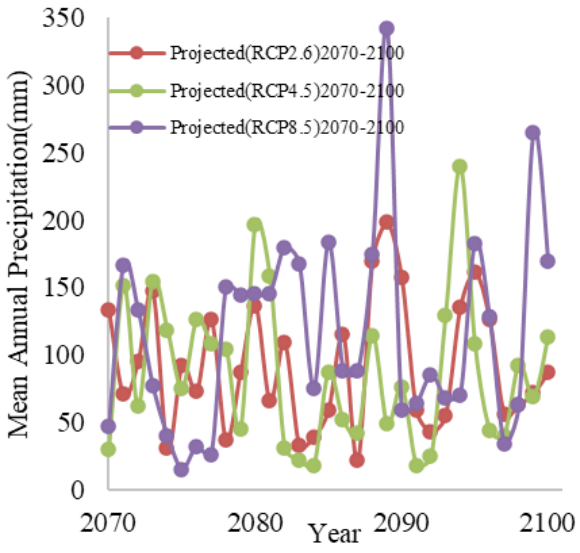

Figure 15. Simulated Rainfall Values for the Far Future Period (2070–2100) at Isfahan Station.

Table 7. Percentage Changes in Annual Average Rainfall Produced Under RCP Scenarios Compared to the Observation Period at Isfahan Station.

Data	Annual average - near future (2030-2060)	Percentage of changes in the near future (2030-2060)	Annual average- far future (2070-2100))	Percentage changes in the far future (2070-2100)
observations	122.05	-	-	-
RCP2.6	92.20	-24.46	92.22	-24.44
RCP4.5	92.14	-24.51	87.09	-28.65
RCP8.5	111.75	-8.44	116.50	-4.55

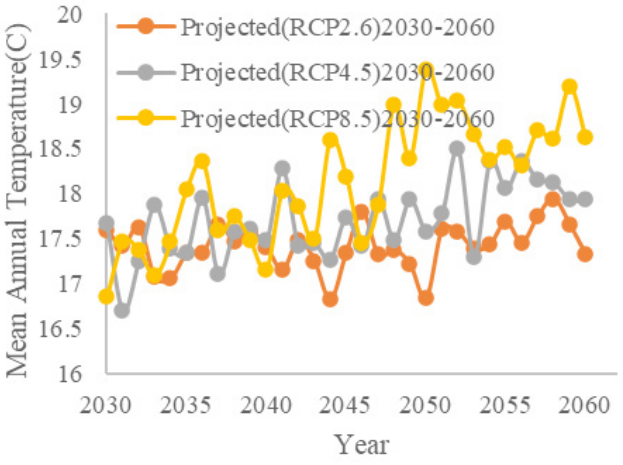

Figure 16. Simulated Average Temperature Values for the Near Future Period (2030–2060) at Isfahan Station.

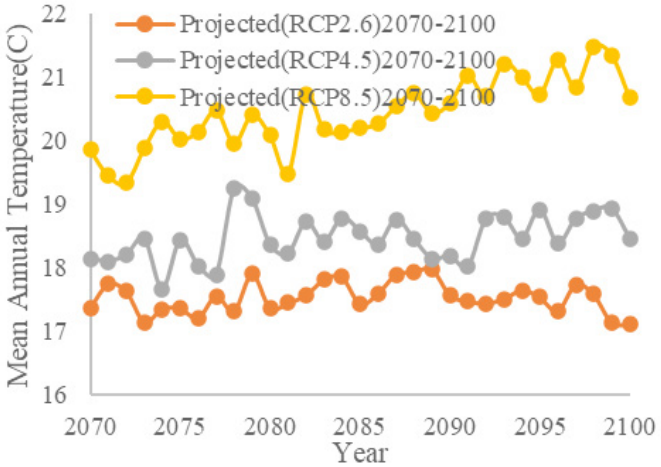

Figure 17. Simulated Average Temperature Values for the Far Future Period (2070–2100) at Isfahan Station.

Table 8. Percentage Changes in Annual Average Temperature Produced Under RCP Scenarios Compared to the Observation Period at Isfahan Station.

Data	Annual average - near future (2030-2060)	Percentage of changes in the near future (2030-2060)	Annual average-far future (2070-2100)	Percentage changes in the far future (2070-2100)
observations	16.69	-	-	-
RCP2.6	17.42	4.39	17.53	5.03
RCP4.5	17.71	6.12	18.47	10.65
RCP8.5	18.13	8.62	20.44	22.43

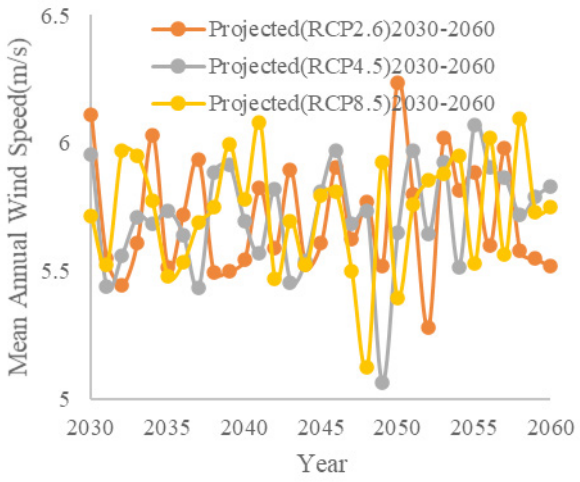

Figure 18. Simulated Wind Speed Values for the Near Future Period (2030–2060) at Isfahan Station.

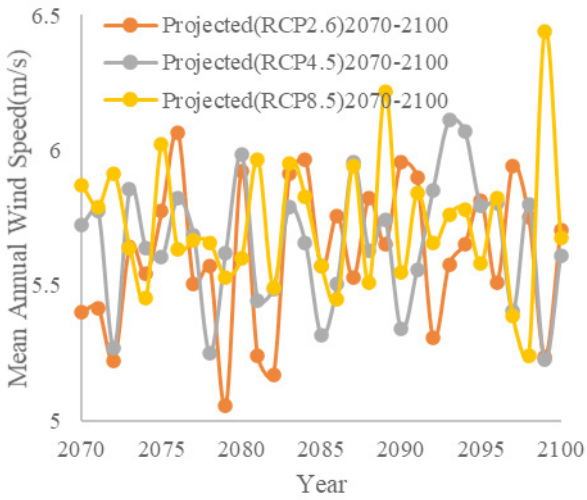

Figure 19. Simulated Wind Speed Values for the Far Future Period (2070–2100) at Isfahan Station.

Table 9. Percentage Changes in Annual Average Wind Speed Produced Under RCP Scenarios Compared to the Observation Period at Isfahan Station.

Data	Annual average - near future (2030-2060)	Percentage of changes in the near future (2030-2060)	Annual average-far future (2070-2100)	Percentage changes in the far future (2070-2100)
observations	5.66	-	-	-
RCP2.6	5.71	1.03	5.62	-0.60
RCP4.5	5.72	1.15	5.66	0.10
RCP8.5	5.73	1.40	5.72	1.31

3.2.2.Kerman Station

Figures 20 to 25 display the simulated future values for climate parameters—rainfall, average temperature, and wind speed. Tables 10 to 12 summarize the changes in these parameters for the near (2030–2060) and far (2070–2100) future periods compared to the historical period. Rainfall simulations indicate that, in the near future, average rainfall under RCP scenarios is projected to be 153.39 mm, 150.43 mm, and 174.13 mm, representing increases of 14.11%, 11.19%, and 29.57% compared to the historical average of 134.41 mm. In the far future, average rainfall under RCP scenarios is expected to reach 155.79 mm, 140.6 mm, and 215.61 mm, indicating increases of 15.91%, 4.60%, and 41.60%, respectively. For temperature, the average values under RCP2.6, RCP4.5, and RCP8.5 scenarios in the near future are projected to be approximately 17.16°C, 17.4°C, and 17.8°C, representing increases of 6.8%, 8.22%, and 10.7% from the observed historical period. In the far future, temperature averages are expected to further rise under RCP scenarios, with projected increases of 17.05%, 18.05%, and 19.93%. Wind speed simulations for Kerman station suggest that wind speeds will increase under RCP scenarios in both the near and far future. In the near future, increases are projected to be 3.71%, 3.9%, and 2.4% for RCP2.6, RCP4.5, and RCP8.5, respectively. In the far future, wind speeds are expected to rise by 2.43%, 3.84%, and 3.97% under the same scenarios.

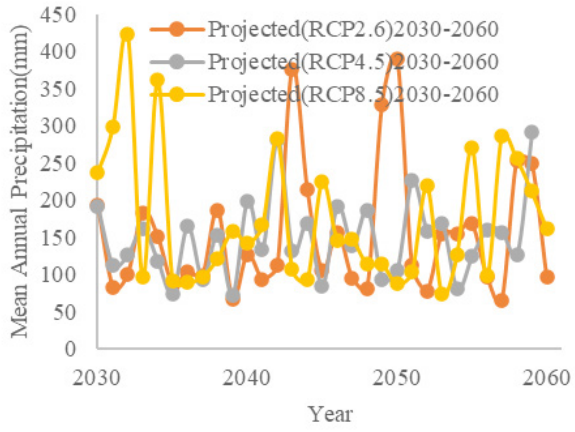

Figure 20. Simulated Rainfall Values for the Near Future Period (2030–2060) at Kerman Station.

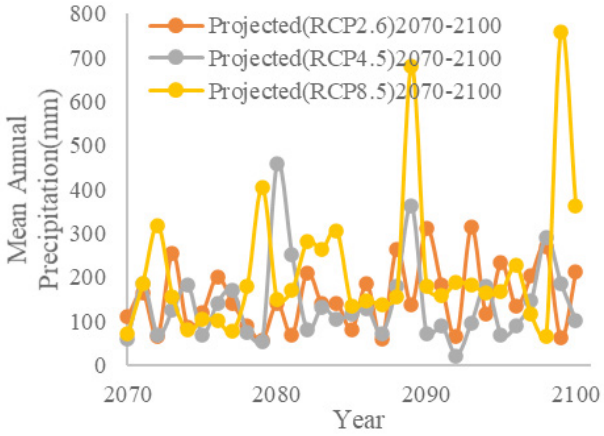

Figure 21. Simulated Rainfall Values for the Far Future Period (2070–2100) at Kerman Station.

Table 10. Percentage Changes in Annual Average Rainfall Produced Under RCP Scenarios Compared to the Observation Period at Kerman Station.

Data	Annual average - near future (2030-2060)	Percentage of changes in the near future (2030-2060)	Annual average-far future (2070-2100)	Percentage changes in the far future (2070-2100)
Observations	134.41	-	-	-
RCP2.6	153.39	14.11	155.79	15.91
RCP4.5	150.43	11.91	140.6	4.60
RCP8.5	174.13	29.57	215.61	60.41

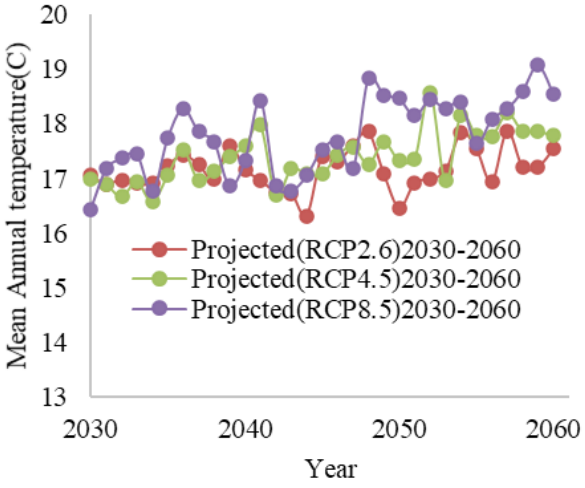

Figure 22. Simulated Average Temperature Values for the Near Future Period (2030–2060) at Kerman Station.

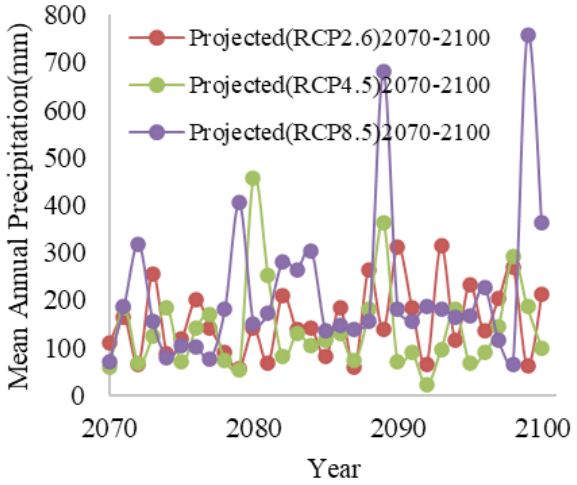

Figure 23. Simulated Average Temperature Values for the Far Future Period (2070–2100) at Kerman Station.

Table 11. Percentage Changes in Annual Average Temperature Produced Under RCP Scenarios Compared to the Observation Period at Kerman Station.

Data	Annual average - near future (2030-2060)	Percentage of changes in the near future (2030-2060)	Annual average-far future (2070-2100)	Percentage changes in the far future (2070-2100)
observations	16.08	-	-	-
RCP2.6	17.16	6.76	17.05	6.08
RCP4.5	17.4	8.22	18.06	12.34
RCP8.5	17.80	10.70	19.93	23.98

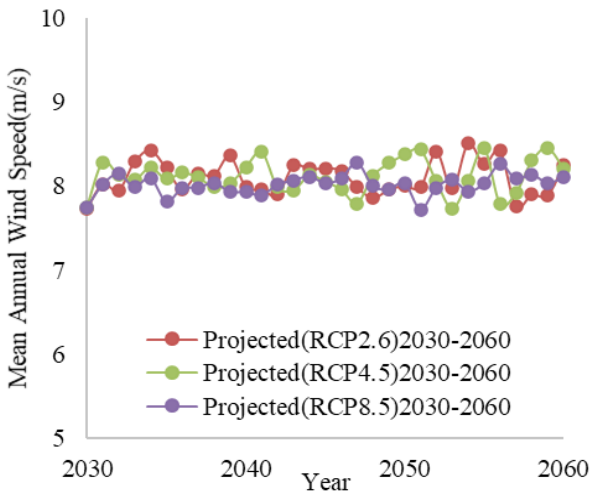

Figure 24. Simulated Wind Speed Values for the Near Future Period (2030–2060) at Kerman Station.

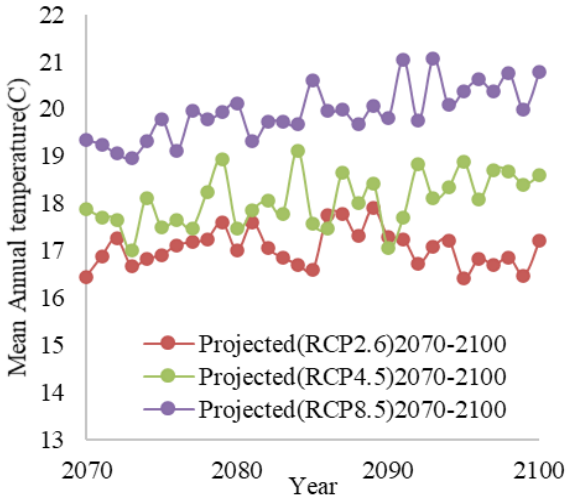

Figure 25. Simulated Wind Speed Values for the Far Future Period (2070–2100) at Kerman Station.

Table 12. Percentage Changes in Annual Average Wind Speed Produced Under RCP Scenarios Compared to the Observation Period at Kerman Station.

Data	Annual average - near future (2030-2060)	Percentage of changes in the near future (2030-2060)	Annual average-far future (2070-2100)	Percentage changes in the far future (2070-2100)
observations	7.81	-	-	-
RCP2.6	8.09	3.71	8.01	2.43
RCP4.5	8.11	3.9	8.11	3.84
RCP8.5	8.01	2.4	8.12	3.97

3.2.3. Semnan Station

The annual mean precipitation and average temperature parameters for Semnan Station during the near future (2030-2060) and far future (2070-2100) periods are presented in Figures 26 to 29. Additionally, Tables 13 and 14 show the changes in these parameters compared to the historical period (1965-2017). Based on the predicted rainfall values, the annual average rainfall for Semnan Station under the RCP scenarios is estimated to be 117.55 mm, 108.72 mm, and 116.5 mm, respectively. This represents a decrease of 14.79%, 21.19%, and 15.55% compared to the historical average of 137.95 mm during the near future period. In the far future, the average rainfall under the RCP scenarios is projected to be 108.8 mm, 110.49 mm, and 104.61 mm, indicating decreases of 21.13%, 19.91%, and 24.17%, respectively, compared to the historical period. Forecasts for average temperature under climate change conditions indicate that, in the near future, the average temperature for the RCP scenarios will be 18.84°C, 18.87°C, and 18.98°C, representing increases of 1.96%, 2.12%, and 2.74%, respectively, compared to the historical value of 18.47°C. In the far future, the average temperature is predicted to be 18.82°C, 19.02°C, and 19.46°C, corresponding to increases of 1.89%, 2.94%, and 5.34%, respectively, compared to the historical period.

3.2.4. Yazd station

The annual averages of precipitation, temperature, and maximum wind speed for the near future (2030–2060) and far future (2070–2100) periods at Yazd Station are shown in Figures 30–35. Tables 15–17 present the changes in these parameters relative to the historical period (1961–2017). Based on projected rainfall values, the annual average rainfall under the RCP scenarios at Yazd Station is estimated to be 64.52, 55.17, and 68.44 mm, representing increases of 17.45%, 0.42%, and 24.58% respectively, compared to the historical period (54.93 mm) for the near future. Forecasts of average temperature under future climate change scenarios indicate that mean temperatures under the RCP scenarios will be 20.79°C, 21.05°C, and 21.56°C, showing increases of 5.45%, 6.77%, and 9.35% respectively, compared to the historical average of 19.71°C. For the far future, average temperatures are predicted to be 21.26°C, 20.67°C, and 21.86°C, corresponding to increases of 7.87%, 4.85%, and 10.9% compared to the historical period.

Model Uncertainty

Although the SDSM and CanESM2 models provide reliable projections, they have inherent limitations. SDSM relies on statistical relationships that may not capture all local microclimatic processes, while CanESM2, as a global climate model, has coarse spatial resolution which can introduce uncertainty in downscaled results. Moreover, variability between RCP scenarios (e.g., RCP2.6 vs. RCP8.5) reflects different emission pathways and assumptions, resulting in a range of possible climate outcomes. Acknowledging these uncertainties is essential for interpreting the projected changes in temperature, rainfall, and wind in Central Iran and for guiding adaptive management strategies.

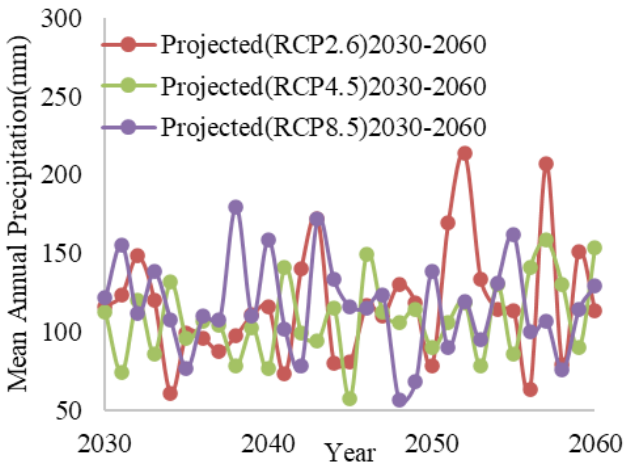

Figure 26. Simulated Rainfall Values for the Near Future Period (2030–2060) at Semnan Station.

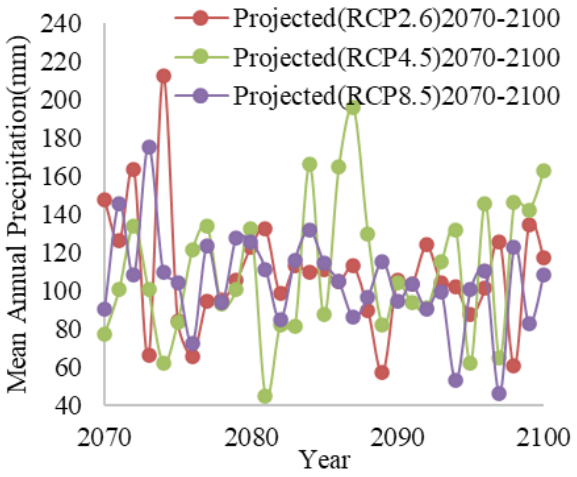

Figure 27. Simulated Rainfall Values for the Far Future Period (2070–2100) at Semnan Station.

Table 13. Percentage of Annual Average Rainfall Changes Under RCP Scenarios Compared to the Observation Period at Semnan Station.

Data	Annual average - near future (2030-2060)	Percentage of changes in the near future (2030-2060)	Annual average-far future (2070-2100)	Percentage changes in the far future (2070-2100)
Observations	137.95	-	-	-
RCP2.6	117.55	-14.79	108.80	-21.13
RCP4.5	108.72	-21.19	110.49	-19.91
RCP8.5	116.50	-15.55	104.61	-24.17

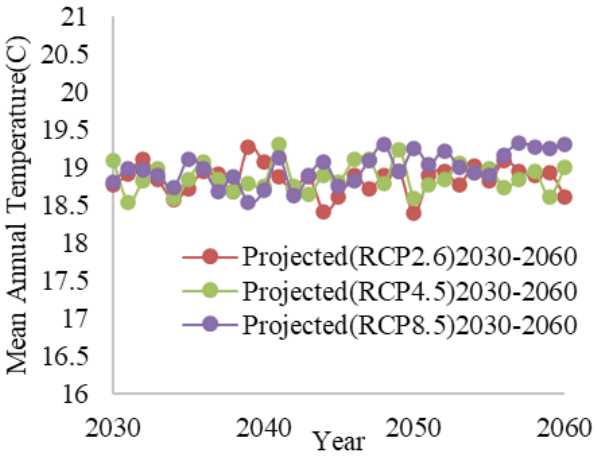

Figure 28. Simulated Average Temperature Values for the Near Future Period (2030–2060) at Semnan Station.

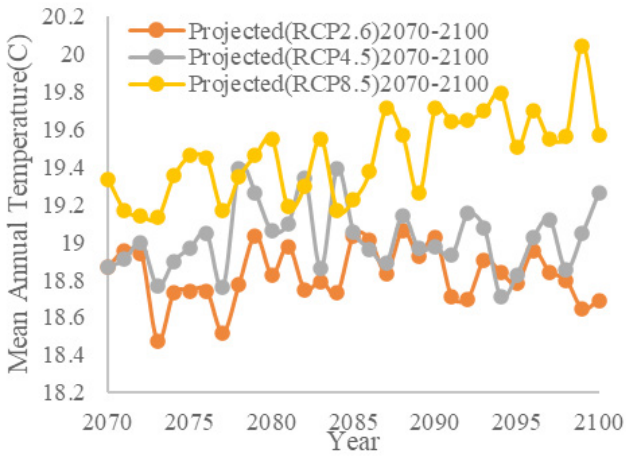

Figure 29. Simulated Average Temperature Values for the Far Future Period (2070–2100) at Semnan Station.

Table 14. Percentage of Annual Average Temperature Changes Under RCP Scenarios Compared to the Observation Period at Semnan Station.

Data	Annual average - near future (2030-2060)	Percentage of changes in the near future (2030-2060)	Annual average-far future (2070-2100)	Percentage changes in the far future (2070-2100)
observations	18.47	-	-	-
RCP2.6	18.84	1.96	18.82	1.89
RCP4.5	18.87	2.12	19.02	2.94
RCP8.5	18.98	2.74	19.46	5.34

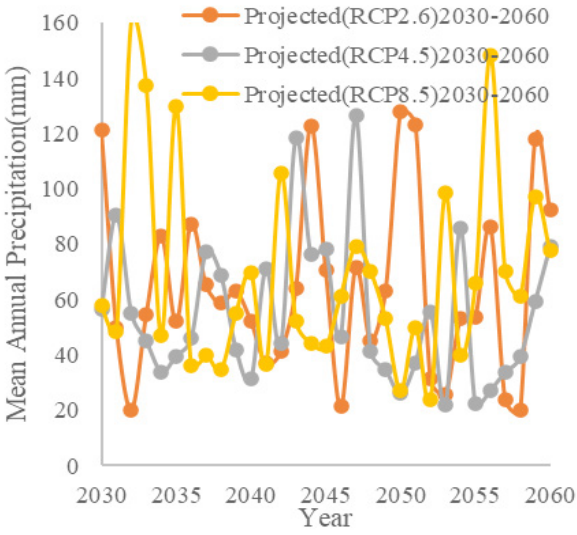

Figure 30. Simulated Rainfall Values for the Near Future Period (2030–2060) at Yazd Station.

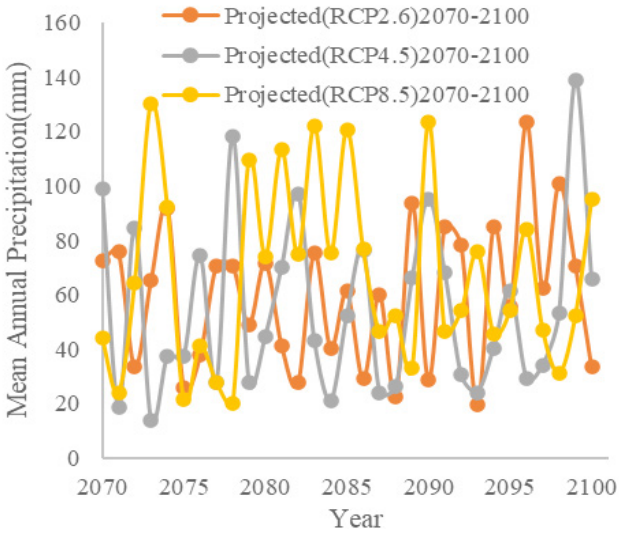

Figure 31. Simulated Rainfall Values for the Far Future Period (2070–2100) at Yazd Station.

Table 15. Percentage Change in Annual Average Rainfall Under RCP Scenarios Compared to the Observation Period at Yazd Station.

Data	Annual average - near future (2030-2060)	Percentage of changes in the near future (2030-2060)	Annual average-far future (2070-2100)	Percentage changes in the far future (2070-2100)
observations	54.93			
RCP2.6	64.52	17.45	60.02	9.25
RCP4.5	55.17	0.42	54.90	-0.07
RCP8.5	68.44	24.58	66.92	21.81

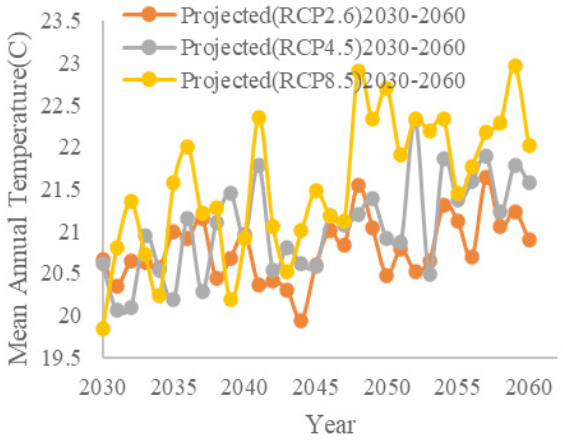

Figure 32. Simulated Average Temperature Values for the Near Future Period (2030-2060) at Yazd Station.

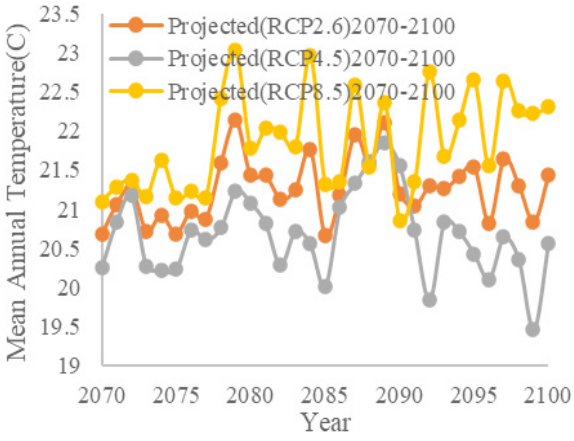

Figure 33. Simulated Average Temperature Values for the Far Future Period (2070-2100) at Yazd Station

Table 16. Percentage of Annual Average Temperature Changes Under RCP Scenarios Compared to the Observation Period at Yazd Station.

Data	Annual average - near future (2030-2060)	Percentage of changes in the near future (2030-2060)	Annual average-far future (2070-2100)	Percentage changes in the far future (2070-2100)
observations	19.71	-	-	-
RCP2.6	20.79	5.45	21.26	7.87
RCP4.5	21.05	6.77	20.67	4.85
RCP8.5	21.56	9.35	21.86	10.90

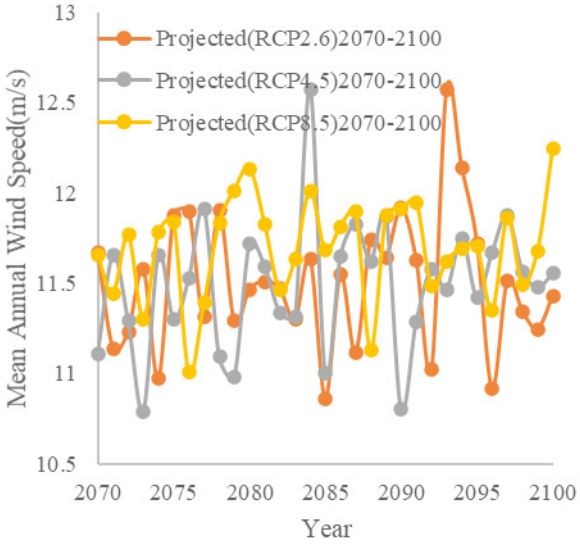

Figure 34. Simulated Wind Speed Values in the Near Future Period (2030-2060) at Yazd Station.

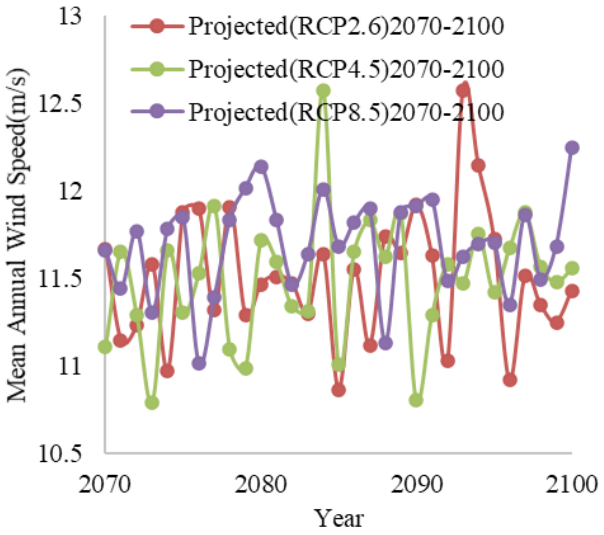

Figure 35. Simulated Wind Speed Values in the Far Future Period (2070-2100) at Yazd Station.

Table 17. Percentage of Annual Average Wind Speed Changes Under RCP Scenarios Compared to the Observation Period at Yazd Station.

Data	Annual average - near future (2030-2060)	Percentage of changes in the near future (2030-2060)	Annual average-far future (2070-2100)	Percentage changes in the far future (2070-2100)
observations	12.73	-	-	-
RCP2.6	11.64	-8.59	11.50	-9.66
RCP4.5	11.48	-9.85	11.49	-9.75
RCP8.5	11.61	-8.79	11.69	-8.17

Discution

Generally, Future simulations were performed under RCP2.6, RCP4.5, and RCP8.5 scenarios, for the near future (2030–2060) and far future (2070–2100). Percent changes in annual averages relative to historical periods are summarized below.

The combination of decreased precipitation and increased temperature for the central and northern stations suggests heightened drought risk. Eastern stations (Kerman, Yazd) may face increased precipitation but higher temperatures, affecting water balance and evaporation.These trends highlight the importance of adaptive water resource management and regional climate planning.

The projected trends for Central Iran, including decreasing precipitation in stations such as Isfahan and Semnan and rising temperatures across all stations, are generally consistent with findings reported in neighboring arid and semi-arid regions. For example, studies in Saudi Arabia indicate reductions in annual rainfall and increased heat stress in recent decades, aligning with the drying trends projected in Central Iran. Similarly, research from India and Pakistan highlights increasing temperatures and variability in monsoon precipitation, which supports the warming and changing rainfall patterns observed in our simulations. These regional comparisons suggest that the climate changes projected for Central Iran are part of broader trends affecting Southwest and South Asia.

In addition, several global projections, including IPCC assessments, indicate that under high-emission scenarios (e.g., RCP8.5), temperature rises are more pronounced, and precipitation patterns become increasingly variable. Our results for the far future (2070–2100) under RCP8.5, showing substantial warming and mixed precipitation trends, are consistent with these broader regional and global projections. By comparing our findings with both regional studies and global models, it becomes evident that the projected climate changes in Central Iran are plausible and reflect patterns observed across similar climatic zones.The projected decrease in rainfall in stations such as Semnan and Isfahan is likely to reduce water availability for irrigation, potentially affecting crop yields and requiring adaptive water management strategies. Conversely, the projected temperature increase in Yazd and surrounding areas will enhance evapotranspiration rates, intensifying water stress and necessitating adjustments in irrigation scheduling, crop selection, and soil moisture conservation practices. These practical implications highlight the need for region-specific adaptation measures to mitigate the impacts of climate change on agriculture and water resources in Central Iran. In general, temperatures are projected to increase across all stations in Central Iran, with the highest rises under the RCP8.5 scenario. Rainfall trends vary regionally: a decrease is observed in the western stations (Isfahan and Semnan), whereas the southern stations (Kerman and Yazd) tend to experience slight increases or smaller decreases in precipitation. Wind speed projections

Table 2. Percentage Changes in Annual Average Precipitation (%)

Station	RCP2.6 2030–2060	RCP4.5 2030–2060	RCP8.5 2030–2060	RCP2.6 2070–2100	RCP4.5 2070–2100	RCP8.5 2070–2100
Isfahan	-24.46	-24.51	-8.44	-24.44	-28.65	-4.55
Kerman	14.11	11.19	29.57	15.91	4.60	41.60
Semnan	-14.79	-21.19	-15.55	-21.13	-19.91	-24.17
Yazd	17.45	0.42	24.58	9.25	-0.07	21.81

Table 3. Percentage Changes in Annual Average Temperature (%)

Station	RCP2.6 2030–2060	RCP4.5 2030–2060	RCP8.5 2030–2060	RCP2.6 2070–2100	RCP4.5 2070–2100	RCP8.5 2070–2100
Isfahan	4.39	6.12	8.62	5.03	10.65	22.43
Kerman	6.76	8.22	10.70	6.08	12.34	23.98
Semnan	1.96	2.12	2.74	1.89	2.94	5.34
Yazd	5.45	6.77	9.35	7.87	4.85	10.90

Table 4. Percentage Changes in Annual Average Wind Speed (%)

Station	RCP2.6 2030–2060	RCP4.5 2030–2060	RCP8.5 2030–2060	RCP2.6 2070–2100	RCP4.5 2070–2100	RCP8.5 2070–2100
Isfahan	1.03	1.15	1.40	-0.60	0.10	1.31
Kerman	3.71	3.90	2.40	2.43	3.84	3.97
Semnan	–	–	–	–	–	–
Yazd	-8.59	-9.85	-8.79	-9.66	-9.75	-8.17

are more variable, with modest increases in Isfahan and Kerman, slight decreases in Yazd, and inconsistent trends in Semnan. These patterns highlight the spatial heterogeneity of climate change impacts within Central Iran and provide a basis for region-specific adaptation strategies.The projected climate changes in Central Iran have important implications for water and agricultural management. Similarly, in Yazd, higher temperatures and enhanced evapotranspiration will exacerbate water stress, necessitating improvements in crop selection, irrigation scheduling, and soil moisture conservation. These findings underline the urgency of integrating climate projections into regional planning and resource management policies.

4. Conclusion

The projected trends for Central Iran, including decreasing precipitation in stations such as Isfahan and Semnan and rising temperatures across all stations, are generally consistent with findings reported in neighboring arid and semi-arid regions. For instance, Almazroui et al. (2020) observed a decrease in annual rainfall in Saudi Arabia, with a significant reduction of 5.89 mm per decade, particularly in the winter months. Similarly, studies in India have highlighted increasing temperatures and variability in monsoon precipitation, indicating a shift towards more extreme rainfall events (He et al., 2024). Research in Pakistan also supports these findings, with Hussain et al. (2024) documenting an increase in monsoon precipitation extremes, particularly in the monsoon region from 1961 to 2017.

This study comprehensively evaluated future changes in temperature, precipitation, and wind speed across Central Iran using the SDSM statistical downscaling model and the CanESM2 global circulation model under RCP2.6, RCP4.5, and RCP8.5 scenarios. The results clearly indicate that temperature is projected to rise by 1.5–4.5°C across all stations, with higher increases expected under RCP8.5 during 2070–2100. Precipitation is projected to decrease by up to 25% in western stations such as Isfahan and Semnan, while the southern regions (Kerman and Yazd) may experience slight increases of up to 10%. Wind speed trends are more spatially variable, with modest increases (1–4%) in Isfahan and Kerman, and slight decreases (up to 9%) in Yazd. These climatic changes are expected to intensify water scarcity, increase irrigation demand, and place additional stress on agricultural systems across this arid and semi-arid region.

The novelty of this research lies in its station-level, multi-variable assessment for Central Iran — a region that has been largely understudied in previous climate modeling efforts. The combination of SDSM and CanESM2 provides more detailed and localized projections, enhancing understanding of how climate change may evolve within Iran's central plateau. The model validation results further confirm the robustness and reliability of the projections, although scenario-based uncertainties remain.

Comparison with regional studies (e.g., Saudi Arabia, India, Pakistan) and global IPCC projections confirms that the observed trends in Central Iran are consistent with broader warming and drying patterns across Southwest and

South Asia. Future research should expand on these findings by integrating socio-economic factors, employing multiple GCMs, and assessing local adaptation strategies such as efficient irrigation, crop diversification, and sustainable land management to strengthen climate resilience in this vulnerable region.

Acknowledgement

The authors of this paper thank the Ministry of Energy of Iran for its cooperation in providing the data required for this research.

References

Almazroui, M., Islam, M. N., & Saeed, S. (2020). Rainfall trends and extremes in Saudi Arabia in recent decades. Atmosphere, 11(9), 964. https://doi.org/10.3390/atmos11090964

Almazroui, M., Nazrul Islam, M., Saeed, F., Alkhalaf, A., & Dambul, R. (2017). Assessing the robustness and uncertainties of projected changes in temperature and precipitation in AR5 Global Climate Models over the Arabian Peninsula. *Atmospheric Research*, 194, 202–213.

Azadi, H., et al. (2018). Farmers' adaptation choices to climate change: A case study of wheat growers in western Iran.Environmental Science & Policy, 87, 1–9.https://doi.org/10.1016/j.envsci.2018.05.007

Bal, P. K., Ramachandran, A., Geetha, R., Bhaskaran, B., Thirumurugan, P., Indumathi, J., & Jayanthi, N. (2016). Climate change projections for Tamil Nadu, India: deriving high-resolution climate data by a downscaling approach using PRECIS. *Theoretical and applied climatology*, 123, 523-535.

Balyani, S., Khosravi, Y., Ghadami, F., Naghavi, M., & Bayat, A. (2017). Modeling the spatial structure of annual temperature in Iran. *Modeling Earth Systems and Environment*, 3(2), 581–593.

Buba, L. F., Kura, N. U., & Dakagan, J. B. (2017). Spatiotemporal trend analysis of changing rainfall characteristics in Guinea Savanna of Nigeria. *Modeling Earth Systems and Environment*, 3(3), 1081–1090.

Cetin, M., Adiguzel, F., & Zeren Cetin, I. (2022). Determination of the effect of urban forests and other green areas on surface temperature in Antalya. In M. N. Suratman (Ed.), *Concepts and Applications of Remote Sensing in Forestry* (pp. 319–336). Springer Nature Singapore.

Cetin, M., Sevik, H., Koc, I., & Zeren Cetin, I. (2023). The change in biocomfort zones in the area of Mugla province in near future due to the global climate change scenarios. *Journal of Thermal Biology*, 112, 103434. https://doi.org/10.1016/j.jtherbio.2022.103434

Cevik Degerli, B., & Cetin, M. (2023). Evaluation of UTFVI index effect on climate change in terms of urbanization. *Environmental Science and Pollution Research International*, 30, 75273–75280. https://doi.org/10.1007/s11356-023-27613-x

Chadwick, R., Boutle, I., & Martin, G. (2013). Spatial patterns of precipitation change in CMIP5: Why the rich do not get richer in the tropics. *Journal of Climate*, 26(11), 3803–3822.

Chen, L., Singh, V. P., Guo, S., Mishra, A. K., & Guo, J. (2013). Drought analysis using copulas. *Journal of Hydrologic Engineering*, 18(7), 797–808.

Chu, J. T., Xia, J., Xu, C. Y., & Singh, V. P. (2010). Statistical downscaling of daily mean temperature, pan evaporation and precipitation for climate change scenarios in Haihe River, China. *Theoretical and Applied Climatology*, 99(1-2), 149-161.

Cong, R.-G., & Brady, M. (2012). The interdependence between rainfall and temperature: Copula analyses. *Scientific World Journal*, 2012, 1–11.

Cooper, J., Dimes, J., Rao, K., Shapiro, B., Shiferaw, B., & Twomlow, S. (2008). Coping better with current climatic variability in the rain-fed farming systems of sub-Saharan Africa: An essential first step in adapting to future climate change? Agriculture, *Ecosystems & Environment*, 126(1-2), 24–35.

Dupuis, D. J. (2007). Using copulas in hydrology: Benefits, cautions, and issues. *Journal of Hydrologic Engineering*, 12(4), 381–393.

Erskine, W., & El Ashkar, F. (1993). Rainfall and temperature effects on lentil (Lens culinaris) seed yield in Mediterranean environments. *Journal of Agricultural Science*, 121(3), 347–354.

Groisman, P. Y., Blyakharchuk, T. A., Chernokulsky, A. V., et al. (2012). Regional environmental changes in Siberia and their global consequences. *In Climate Changes in Siberia*. Springer.

Gupta, S. K., & Dutta, S. (2021). Spatiotemporal assessment of climate change in rainfall and temperature patterns in a North-East Himalayan state of India. *Atmospheric Science Letters*, 22(5), e1012. https://doi.org/10.1002/asl.1012

Hawkins, E., Frame, D., Harrington, L., Joshi, M., King, A., Rojas, M., & Sutton, R. (2020). Observed emergence of the climate change signal: From the familiar to the unknown. *Geophysical Research Letters*, 47(6), e2019GL086259. https://doi.org/10.1029/2019GL086259

He, J., Zhang, L., & Wang, H. (2024). Opposing changes in Indian summer monsoon rainfall and its variability. Geophysical Research Letters. https://doi.org/10.1029/2024GL109897

Hussain, A., Ali, A., & Ahmad, S. (2024). Increasing monsoon precipitation extremes in relation to climate change in Pakistan. Science of the Total Environment, 2024, 123456. https://doi.org/10.1016/j.scitotenv.2024.123456

IPCC. (2021). Climate Change 2021: The Physical Science Basis. Contribution of Working Group I to the Sixth Assessment Report of the Intergovernmental Panel on Climate Change. Cambridge University Press. https://doi.org/10.1017/9781009157896

Keerthirathne, D. G. T. C., & Perera, K. (2015). Joint distribution of rainfall and temperature in Anuradhapura, Sri Lanka using copulas. *In Proceedings of the International Research Symposium on Engineering Advancements (RSEA 2015)* (pp. 1-8). SAITM.

Kharin, V. V., Zwiers, F. W., Zhang, X., & Wehner, M. (2013). Changes in temperature and precipitation extremes in the CMIP5 ensemble. *Climatic Change*, 119(2), 345–357.

Khosravi, Y., Balyani, S., & Ghadami, F. (2020). Evaluation of spatiotemporal patterns of annual precipitation in Iran based on copula theory. *Theoretical and Applied Climatology*, 140(3-4), 1047-1059.

Kreyling, J., & Beier, C. (2013). Complexity in climate change manipulation experiments. *Bioscience*, 63(9), 763–767.

Lobell, D., & Field, C. (2007). Global scale climate-crop yield relationships and the impacts of recent warming. *Environmental Research Letters*, 2(1), 014002.

Mahmood, R., & Babel, S. M. (2012). Evaluation of SDSM developed by annual and monthly sub-models for downscaling temperature and precipitation in the Jhelum basin, Pakistan and India. *Theoretical and Applied Climatology*, 113(1-2), 1-18. https://doi.org/10.1007/s00704-012-0763-2

Marin, M., Clinciu, I., Tudose, N. C., Ungurean, C., Adorjani, A., Mihalache, A. L., Davidescu, A. A., Davidescu, Ş. O., Dinca, L., & Cacovean, H. (2020). Assessing the vulnerability of water resources in the context of climate changes in a small forested watershed using SWAT: A review. *Environmental Research*, 184, 109330. https://doi.org/10.1016/j.envres.2020.109330

Muchow, R., Sinclair, T., & Bennett, J. (1999). Temperature and solar-radiation effects on potential maize yield across locations. *Agronomy Journal*, 82(2), 338–343.

Pandey, P. K., Das, L., Jhajharia, D., & Pandey, V. (2018). Modelling of interdependence between rainfall and temperature using copula. *Modeling Earth Systems and Environment*, 4(2), 867–879.

Sethi, R., Pandey, B. K., Krishan, R., Khare, D., & Nayak, P. C. (2015). Performance evaluation and hydrological trend detection of a reservoir under climate change condition. *Modeling Earth Systems and Environment*, 1(4), 1–11.

Shaban, A., et al. (2021). Assessment of climate variations in temperature and precipitation over Iran.Theoretical and Applied Climatology, 143(3–4), 1–14.https://doi.org/10.1007/s00704-020-03389-2

Sutton, R., Suckling, E., & Hawkins, E. (2015). What does global mean temperature tell us about local climate? *Philosophical Transactions of the Royal Society A*, 373(2054), 20140426. https://doi.org/10.1098/rsta.2014.0426

Tabari, H., & Hosseinzadeh Talaee, P. (2016).Climate change impact on water resources in Iran.Environmental Earth Sciences, 75(6), 1–13.https://doi.org/10.1007/s12665-016-5484-1

Tabari, H., et al. (2015). Climate change projections for temperature and precipitation in Iran's central plateau.Theoretical and Applied Climatology, 120(1–2), 1–12. https://doi.org/10.1007/s00704-014-1234-5

Tabari, H., Marofi, S., Aeini, A., Hosseinzadeh Talaee, P., & Mohammadi, K. (2011). Trend analysis of reference evapotranspiration in the western half of Iran. *Agricultural and Forest Meteorology*, 151(2), 128-136.

Varol, T., Cetin, M., Altan, S., & Bahattin, K. (2022). The effect of forest fires on land cover change in Marmara Region, Turkey. *Science of The Total Environment*, 815, 152908. https://doi.org/10.1016/j.scitotenv.2021.152908

Wang, J., Hu, X., Ma, J., Wang, X., & Yang, X. (2021). Spatiotemporal variability of temperature and precipitation and its impact on potential evaporation in the Yellow River basin. *Theoretical and Applied Climatology*, 143(3-4), 1079-1092.

Wang, Q., Wang, G., & Liu, L. (2021). Research progress on the influence of climate change on extreme weather and climate events in China. *Climate*, 9(11), 150.

Wang, X. L., Feng, Y., Compo, G. P., Swail, V. R., Zwiers, F. W., Allan, R. J., & Sardeshmukh, P. D. (2013). Trends and low frequency variability of extra-tropical cyclone activity in the ensemble of the Twentieth Century Reanalysis. *Climate Dynamics*, 40, 2775–2800. https://doi.org/10.1007/s00382-012-1450-9

Wang, Y., Jiang, T., Bothe, O., & Fraedrich, K. (2007). Changes of pan evaporation and reference evapotranspiration in the Yangtze River basin. *Theoretical and Applied Climatology*, 90, 13-23.

Yang, Y., Huang, G., & Zhao, Y. (2022). Impacts of climate change on the frequency and intensity of extreme precipitation events in China: A literature review. *International Journal of Climatology*, 42(5), 2986–3006.

Zhang, W., Chen, C., Yang, H., & Zhao, Q. (2022). Analysis of the relationship between precipitation and temperature in arid and semi-arid regions: A case study of the Inner Mongolia of China. *Theoretical and Applied Climatology*, 148(1-2), 507–518.